Inorg. Chem. **2006**, *45*, 6628–6636

Neutral and Cationic Complexes with P-Bonded 2-Pyridylphosphines as N-Donor Ligands toward Rhodium. Electrical Charge vs Steric Hindrance on the Conformational Control

Juan A. Casares, Pablo Espinet,* José M. Martín-Álvarez, and Verónica Santos

Química Inorgánica, Facultad de Ciencias, Universidad de Valladolid, E-47071 Valladolid, Spain

Received January 10, 2006

Bimetallic palladium(II)–rhodium(I) and gold(I)–rhodium(I) complexes of the type [(4,4′-Me_2-bipy)(C_6F_5)Pd(μ-$PPh_{3-n}Py_n$)Rh(diene)](BF_4)$_2$ and [(C_6F_5)Au(μ-$PPh_{3-n}Py_n$)Rh(diene)](BF_4) (n = 2, 3; Py = 2-pyridyl) have been synthesized. The P donor atom of the bridging ligands (μ-$PPh_{3-n}Py_n$) is coordinated to the Pd or to the Au center. The resulting complexes react with [Rh(diolefin)(solv)$_2$]$^+$ (solv = acetone) in a way similar to pyrazolylborates, affording square-planar or pentacoordinated rhodium complexes with two or the three N-donor ends chelating the Rh atom. The metallacycles formed upon chelation can adopt one of two conformations in the square-planar Rh(I) complexes, either bringing the other metal close to the Rh center or bringing it to a remote position. The first conformation is preferred for the gold P-coordinated complexes and the second for the palladium complexes. The X-ray structures of [(4,4′-Me_2-bipy)](C_6F_5)Pd(μ-$PPhPy_2$)Rh(COD)](BF_4)$_2$ (COD = 1,5 cyclooctadiene) and [Au(C_6F_5)(μ-$PPhPy_2$)Rh-(TFB)](BF_4) (TFB = 5,6,7,8-tetrafuoro-1,4-dihydro-1,4-etenonaphthalene) are reported.

Introduction

The coordination chemistry of the 2-pyridylphosphines is currently a topic of great interest that has been extensively reviewed.[1] Most studies have been concerned with PPh_2Py (Py = 2-pyridyl), which is a useful building block for the synthesis of homo- or hetero-bimetallic compounds because the rigidity induced by the small bite angle of the ligand favors the formation of M−M bonds. The synthetic relevance of this strategy was early recognized by Balch and co-workers, and it continues to be a useful synthetic tool.[2,3] On the other hand, the different electronic properties for P and N donor atoms facilitate chemoselective bonding of the ligand in molecules with both hard and soft metal centers. The coordination chemistry of the related ($PPhPy_2$) and tetradentate (PPy_3) ligands has been much less studied, but there are a few reports on their catalytic application as amphiphilic water-soluble ligands and as proton carriers.[4−6]

As a part of our ongoing research on complexes with pyridylphosphines and their derivatives,[4,7] we have studied before heterobimetallic complexes with $PPhPy_2$ and PPy_3 as

* To whom correspondence should be addressed. E-mail: espinet@qi.uva.es.

(1) (a) Espinet, P.; Soulantica, K. *Coord. Chem. Rev.* **1999**, 499−556. (b) Zhang, Z. Z.; Cheng, H. *Coord. Chem. Rev.* **1996**, *147*, 1−39. (c) Newkome, G. R. *Chem. Rev.* **1993,** *93*, 2067−2089.

(2) See for instance: (a) Olmstead, M. M.; Maisonnet, A.; Farr, J. P.; Balch, A. L. *Inorg. Chem.* **1981**, *20*, 4060. (b) Farr, J. P.; Olmstead, M. M.; Balch, A. L. *Inorg. Chem.* **1983**, *22*, 1229. (c) Zang, Z.-Z.; Wang, H.-K.; Wang, H.-G. *J. Organomet. Chem.* **1986**, *314*, 357. (d) Farr, J. P.; Olmstead, M. M.; Wood, F. D.; Balch, A. L. *J. Am. Chem. Soc.* **1983**, *105*, 792.

(3) For recent reports on the use of pyridylphosphines as bridging ligands see: (a) Zhang, T. L.; Chen, C. G.; Qin, Y.; Meng, X. G. *Inorg. Chem. Commun.* **2006**, *9* (1), 72−74. (b) Zhang, T. L.; Qin, Y.; Wu, D. Y.; Liu, C. L. *J. Coord. Chem.* **2005**, *58*, 1485−1491. (c) Li, Q. S.; Xu, F. B.; Cui, D. J.; Yu, K.; Zeng, X. S.; Leng, X. B.; Song, H. B.; Zang, Z. Z. *Dalton Trans.* **2003**, *8*, 1551−1557. (d) Driess, M.; Franke, F.; Merz, K. *Eur. J. Inorg. Chem.* **2001**, *10*, 2661−2668.

(4) (a) Pruchnik, F. P.; Smolenski, P.; Wajda-Hermanowicz, K. *J. Organomet. Chem.* **1998**, *570*, 63−69. (b) Buhling, A.; Kamer, P. C. J.; van Leeuwen, P. W. N. M.; Elgersma, J. W. *J. Mol. Catal. A: Chem.* **1997**, *116*, 297−308. (c) Baird, I. R.; Smith, M. B.; James, B. R. *Inorg. Chim. Acta* **1995**, *235*, 291−297. (d) Buhling, A.; Kamer, P. C. J.; van Leeuwen, P. W. N. M. *J. Mol. Catal. A: Chem.* **1995**, *98*, 69−80 (e) Drent, E.; Arnoldy, P.; Budzelaar, P. H. M. *J. Organomet. Chem.* **1993**, *455*, 247 (f) Xie, Y.; Lee, C.-L.; Yang, Y.; Rettig, S. J.; James, B. R. *Can. J. Chem.* **1992**, *70*, 751−756.

(5) (a) Schutte, R. P.; Rettig, S. J.; Joshi, A. J.; James, R. J. *Inorg. Chem.* **1997**, *36*, 5809−5817. (b) Wajda-Hermanowicz, K.; Pruchnik, F.; Zuber, M. *J. Organomet. Chem.* **1996**, *508*, 75−81.

(6) (a) Espinet, P.; Hernando, R.; Iturbe, G.; Villafañe, F.; Orpen, A. G.; Pascual, I. *Eur. J. Inorg. Chem.* **2000**, *5*, 1031−1038. (b) Casares, J. A.; Espinet, P.; Hernando, R.; Iturbe, G.; Villafañe, F. *Inorg. Chem.* **1997**, *36*, 44−49.(c) Espinet, P.; Gómez-Elipe, P.; Villafañe, F. *J. Organomet. Chem.* **1993**, *450*, 145−150.

(7) (a) Alonso, M. A.; Casares, J. A.; Espinet, P.; Martínez-Ilarduya, J. M.; Pérez-Briso, C. *Eur. J. Inorg. Chem.* **1998**, 1745−1753. (b) Casares, J. A.; Espinet, P.; Martínez de Ilarduya, J. M.; Lin, Y.-S. *Organometallics* **1997**, *16*, 770−779. (c) Casares, J. C.; Coco, S.; Espinet, P.; Lin, Y.-S. *Organometallics* **1995**, *14*, 3058−3067. (d) Casares, J. A.; Espinet, P.; Martín-Alvarez, J. M.; Espino, G.; Pérez-Manrique, M.; Vattier, F. *Eur. J. Inorg. Chem.* **2001**, 289−296.

10.1021/ic0600477 CCC: $33.50
Published on Web 07/27/2006

Chart 1

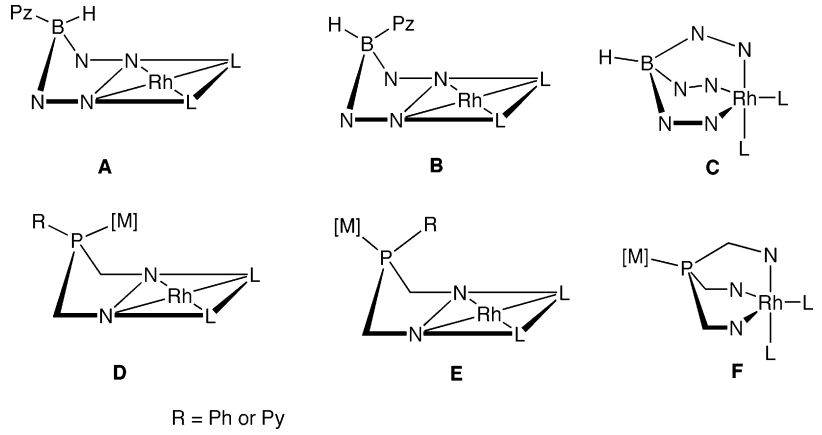

Scheme 1

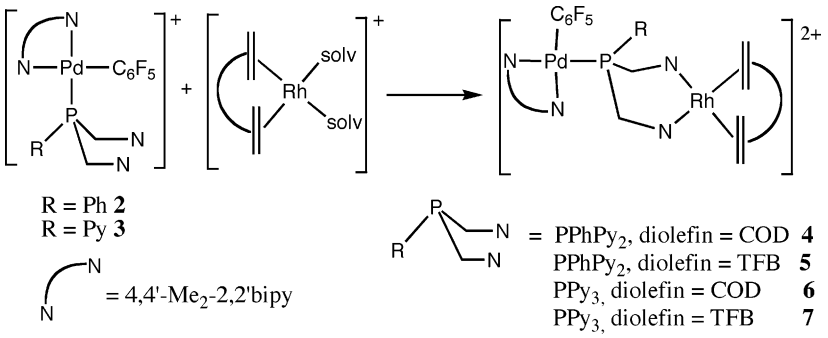

bridging ligands.[4,8,9] In complexes where the pyridyl groups coordinate a "[Rh(diolefin)]$^+$" fragment (once the P functionality has been blocked by oxidation or by coordination to a soft metal to form a metaloligand), the conformational behavior of the resulting chelated ligand can be compared to that of pyrazolylborate ligands (Chart 1). Complexes Tp′ML_2 (M = Rh(I), Ir(I)) display κ^2 or κ^3 coordination modes depending on the nature of the Tp′ ligand, the metal, and the coligands. While κ^3 coordination yields 18-electron trigonal bipyramidal structures (complexes **C** in Chart 1), κ^2 binding results in 16-electron square-planar species. In the latter, the different substituents at the boron can be oriented in pseudoequatorial or pseudoaxial positions in the boat defined by the chelate, giving rise to different conformers (**A** or **B** in Chart 1). These aspects, well studied in pyrazolylborate chemistry,[10,11] have been also examined before for complexes with the metaloligands $[Pt(C_6F_5)_3(PPh_{3-n}Py_n)]^-$ (n = 2, 3), where other features not present in the Tp′ systems, such as the charge on the metals and the remarkable bulk of $[Pt(C_6F_5)_3(PPy_n)]^-$, are involved.[9] Structures **D** and **E**, similar to **A** and **B** in the Tp′ system, were found. In this work, we examine the behavior of complexes [M](μ-$PPh_{3-n}Py_n$)Rh(diolefin) (n = 2, 3; diolefin = norbornadiene, tetrafluorobenzobarrelene (TFB, 5,6,7,8-tetrafuoro-1,4-dihydro-1,4-etenonaphthalene)) in which the metal fragment participating in the metaloligand, [M], is neutral Au(C_6F_5) or cationic $[Pd(C_6F_5)(4,4'\text{-}Me_2\text{-bipy})]^+$ instead of anionic $[Pt(C_6F_5)_3]^-$.

Results and Discussion

Synthesis of the Complexes. Complexes $[Pd(C_6F_5)(4,4'\text{-}Me_2\text{-bipy})(PPhPy_2)](BF_4)$ (**2**) and $[Pd(C_6F_5)(4,4'\text{-}Me_2\text{-bipy})(PPy_3)](BF_4)$ (**3**) were prepared by substitution of bromide by $PPhPy_2$ or PPy_3 in the precursor $[Pd(C_6F_5)Br(4,4'\text{-}Me_2\text{-bipy})]$ (**1**). These cationic complexes were used as N-donor ligands toward $[Rh(diolefin)(solv)_2]^+$ (solv = solvent), which were prepared in situ, affording the dicationic Pd/Rh complexes **4**−**7** (Scheme 1). In a similar way the neutral gold(I) complexes $[Au(C_6F_5)(PPhPy_2)]$ (**8**) and $[Au(C_6F_5)(PPy_3)]$ (**9**) were used to prepare the monocationic Au/Rh complexes **10**−**13** (Scheme 2).

As discussed below, all complexes **4**-**7** have a type **E** structure (Chart 1) in the solid state and in solution, keeping the two cationic metal centers separated, while all complexes **10**-**12** prefer a type **D** structure. Only **13** shows in solution a mixture of two isomers with structures **F** (major) and **D** (minor). The X-ray structures of **4** and **11** were studied.

Solid-State Structures. $[(4,4'\text{-}Me_2\text{-bipy})(C_6F_5)Pd(\mu\text{-}PPhPy_2)Rh(COD)](BF_4)_2$ (4). The solid-state structure of

(8) (a) Alonso, M. A.; Casares, J. A.; Espinet, P.; Soulantica, K.; Charmant, A. G.; Orpen, A. G. *Inorg. Chem.* **2000**, *39*, 705−711. (b) Casares, J. A.; Espinet, P.; Soulantica, K.; Pascual, I.; Orpen, A. G. *Inorg. Chem.* **1997**, *36*, 5251..

(9) Casares, J. A.; Espinet, P.; Martín-Álvarez, J. M.; Santos, V. *Inorg. Chem.* **2004**, *43*, 189−197.

(10) (a) Trofimenko, S. *Chem. Rev.* **1993**, *93*, 943−980. (b) Kitajima, N.; Tolman, W. B. *Prog. Inorg. Chem.* **1995**, *43*, 419−531. (c) Slugovc, C.; Padilla-Martínez, I.; Sirol, S.; Carmona, E. *Coord. Chem. Rev.* **2001**, *213*, 129−157.

(11) (a) Bucher, U. E.; Currao, A.; Nesper, R.; Rüeger, H.; Venanzi, L. M.; Younger, E. *Inorg. Chem.* **1995**, *34*, 66−74. (b) Sanz, D.; Santa-María, M. D.; Claramunt, R. M.; Cano, M.; Heras, J. V.; Campo, J. A.; Ruíz, F. A.; Pinilla, E.; Monge, A. *J. Organomet. Chem.* **1996**, *526*, 341−350.

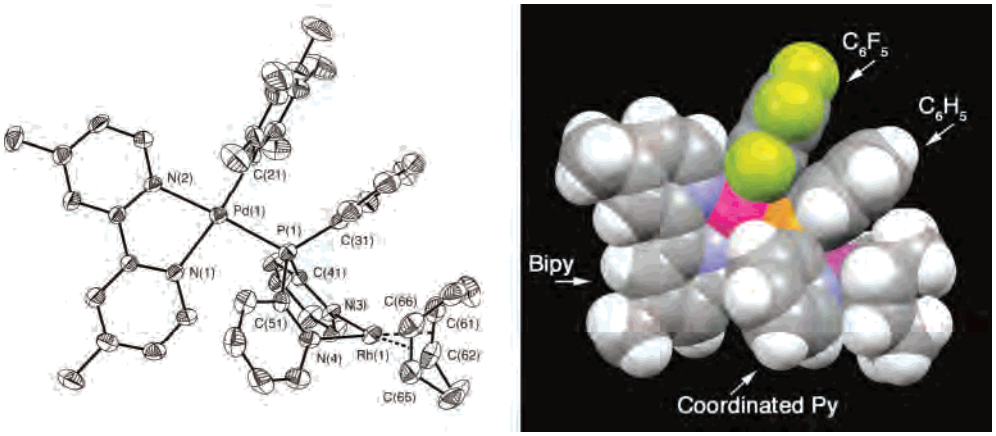

Figure 1. Left, ORTEP representation of the cation of complex **4**. Right, space-filling representation showing how one bipy ring is forced inside the cleft between the two coordinated Py groups.

Table 1. Selected Distances [Å] and Angles [deg] of the Cation of Complex **4**, $[(4,4'\text{-}Me_2Bipy)(C_6F_5)Pd(\mu\text{-}PPhPy_2)Rh(COD)]^{2+a}$

Pd(1)−C(21)	1.999(5)	C(21)−Pd(1)−N(2)	94.22(16)
Pd(1)−N(2)	2.083(4)	C(21)−Pd(1)−N(1)	172.96(17)
Pd(1)−N(1)	2.104(3)	N(2)−Pd(1)−N(1)	78.82(14)
Pd(1)−P(1)	2.2526(14)	C(21)−Pd(1)−P(1)	88.04(14)
N(3)−Rh(1)	2.110(4)	N(2)−Pd(1)−P(1)	175.00(12)
N(4)−Rh(1)	2.093(4)	N(1)−Pd(1)−P(1)	98.98(11)
Rh(1)-M(1)	2.013(6)	N(4)−Rh(1)−N(3)	87.50(15)
Rh(1)-M(2)	2.014(6)	KPy(1)−KPy(2)	61.93(12)
Rh(1)−P(1)	3.375(5)		
Rh(1)−Pd(1)	5.570(4)		

[a] M1 and M2 are C61−C62 and C65−C66 centroids. KPy(1)−KPy(2) are the planes where the pyridyl groups are located.

Scheme 2

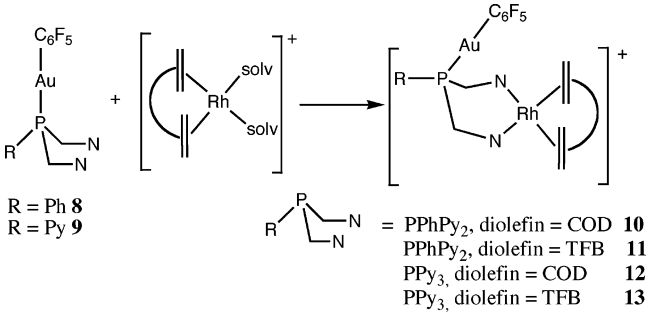

R = Ph **8**
R = Py **9**

P, R, N, N = PPhPy$_2$, diolefin = COD **10**
PPhPy$_2$, diolefin = TFB **11**
PPy$_3$, diolefin = COD **12**
PPy$_3$, diolefin = TFB **13**

the cation of complex **4** is shown in Figure 1, and selected bond distances and angles are given in Table 1.

The metallic centers, palladium and rhodium, are located in square-planar coordination environments, with bond distances and angles within the range of normal values.[15] The two coordination planes are almost perpendicular (82.89(5)°). The ligand 4,4′-Me_2-bipy is on the palladium coordination plane and shows a small bite angle (78.82(14)°). The C_6F_5 ring is almost perpendicular to the palladium coordination plane, as usually found, and almost parallel to the P−Ph ring, with a distance of 3.695(8) Å between the corresponding centroids. The proximity between these two aromatic rings can be expected to hinder their rotation about the C−P and C−Pd bonds, but due to the symmetry expected for **4** in solution (where the Pd coordination plane should become a symmetry plane), this hindrance cannot be confirmed nor disproved by NMR spectroscopy. However, the hindrance to rotation about the P−C bond has been confirmed for the sterically equivalent **6** (see below).

The chelate formed by the two Py groups coordinated to rhodium shows a boatlike conformation of type **E** (Chart 1) with the $[Pd(C_6F_5)(4,4'\text{-}Me_2\text{-bipy})]^+$ fragment occupying the pseudoequatorial position and the phenyl group in the pseudoaxial one. This conformation forces the P-pyridyl groups to adopt a bite angle slightly smaller than 90°, as often found in other complexes with these ligands.[4a,7] On the other hand, the angle between the two 2-pyridyl rings (61.93(12)°) is forced here to be larger than usual because of the steric requirement of one pyridyl ring of the 4,4′-Me_2-bipy group, which is sandwiched between them. For comparison, the angle found in the zwitterionic complex $[Pt(C_6F_5)_3(\mu\text{-}PPhPy_2)Rh(COD)]$, without any fragment slotted in the space between the 2-pyridyl rings, is 51.59(11)°.[9]

$[Au(C_6F_5)(\mu\text{-}PPhPy_2)Rh(TFB)](BF_4)$ (11). The structure of the cation of complex **11** is shown in Figure 2 and the selected bond distances and angles are given in Table 2.

The rhodium atom is in a square-planar coordination environment, while the gold atom has a distorted linear coordination with a C−Au−P angle of 167.8(3)° due to the clash between the C_6F_5 ring and the TFB ligand of a neighboring cation, as can be seen in Figure 3. The chelate formed by the two Py groups coordinated to rhodium

(12) See, for instance: (a) Alonso, M. A.; Casares, J. A.; Espinet, P.; Soulantica, K.; Orpen, G.; Phetmung, H. *Inorg. Chem.* **2003**, *42*, 3856−3864. (b) Haarman, H. F.; Ernsting, J. M.; Kranenburg, M.; Kooijman, H.; Veldamn, N.; Spek, A. L.; van Leeuwen, P. W. N. M. *Organometallics* **1997**, *16*, 887. (c) Heitner, H. I.; Lippard, S. J. *Inorg. Chem.* **1972**, *11*, 1447. (d) Vrieze, K.; van Leeuwen, P. W. N. M. Prog. *Inorg. Chem.* **1971**, *14*, 1. (e) Heitner, H. I.; Lippard, S. *J. Am. Chem. Soc.* **1970**, *92*, 3486.

(13) Proposals of dissociation of a nonolefinic ligand can be found in: (a) Yoshida, T.; Tani, K.; Yamagata, T.; Tatsuno, Y.; Saito, T. *J. Chem. Soc. Chem. Commun.* **1990**, 292−294. (b) Berger, H.; Nesper, R.; Pregosin, P. S.; Rüegger, H.; Wörle, M. *Helv. Chim. Acta* **1993**, *76*, 1520. (c) Yang, H.; Lugan, N.; Mathieu, R. *Organometallics* **1997**, *16*, 2089. (d) Valentini, M.; Selvakumar, K.; Wörle, M.; Pregosin, P. S. *J. Organomet. Chem.* **1999**, *587*, 244−251. (e) Selvakumar, K.; Valentini, M.; Pregosin, P. S. *Organometallics* **2000**, *19*, 1299.

(14) The dissociation of one olefin has also been proposed: (a) Crociani, B.; Antonaroli, S.; Di Vona, M. L.; Licoccia, L. *J. Organomet. Chem.* **2001**, *631*, 117−124.

(15) Line shape analysis was carried out using the standard gNMR program: Budzelaar, P. H. M. *gNMR*; Cherwell Scientific Publishing Ltd.: Oxford, U.K.

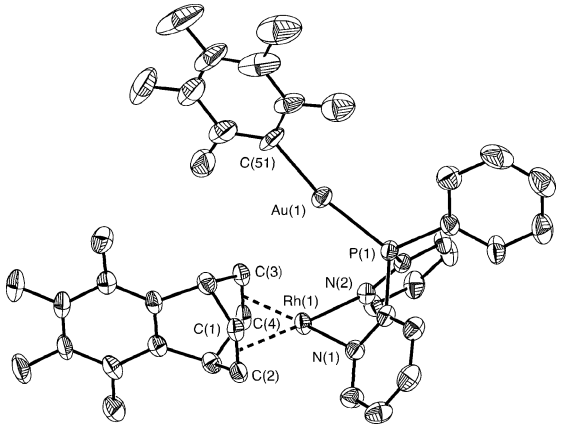

Figure 2. ORTEP representation of the cation **11**.

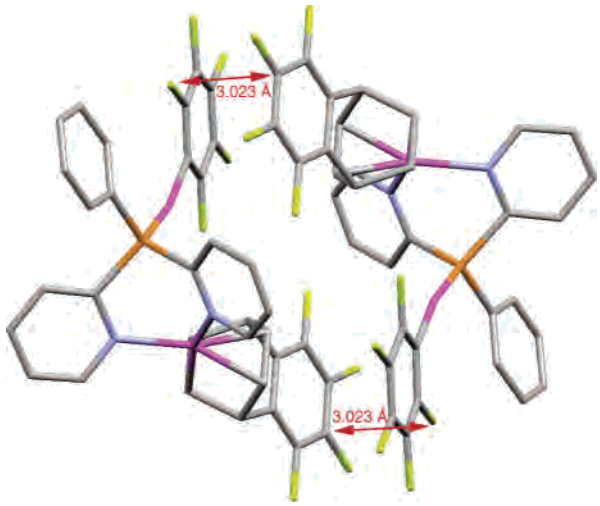

Figure 3. Representation of the packing of two neighboring cations of complex **11**.

Table 2. Selected Distances [Å] and Angles [deg] of the Cation of Complex **11**, $[(C_6F_5)Au(\mu\text{-}PPhPy_2)Rh(TFB)]^{+a}$

Rh(1)−N(2)	2.096(6)	N(2)−Rh(1)−N(1)	89.0(2)
Rh(1)−N(1)	2.116(6)	C(51)−Au(1)−P(1)	167.8(3)
Rh(1)−M(1)	2.002(5)	KPy(1)−KPy(2)	63.2(3)
Rh(1)−M(2)	2.020(5)		
Rh(1)−P(1)	3.214(5)		
Au(1)−P(1)	2.2684(18)		
Au(1)−C(51)	2.060(8)		
Au(1)−Rh(1)	3.736(5)		

[a] M1 and M2 are C1−C2 and C3−C4 centroids. KPy(1)−KPy(2) are the planes where the pyridines are located.

describes a boatlike conformation of type **D** (Chart 1) with the $Au(C_6F_5)$ group in the axial position. The phenyl group is in the equatorial position and is contained in the plane bisecting the dihedral angle between the two Py groups, perpendicular to the rhodium coordination plane. The line connecting the gold and rhodium atoms (which are at a noninteraction distance of 3.736(5) Å) is almost perpendicular to the rhodium coordination plane. The orientation of the C_6F_5 ring, almost perpendicular to the rhodium coordination plane, is due to packing forces, not to intramolecular interactions.

Solution Behavior. Dicationic Complexes with the $[Pd(C_6F_5)(4,4'\text{-}Me_2\text{-}bipy)]^+$ Fragment, 4−7. Table 3 summarizes the most relevant spectroscopic data of complexes **4**−**13** in solution. The dicationic complexes **4**−**7** maintain in solution the conformation found in the solid state (conformation **E** in Chart 1). No other conformers are detected. Accordingly, only one signal is observed in their ^{31}P NMR spectra. Interestingly, in the related compounds $[(C_6F_5)_3Pt(\mu\text{-}PPhPy_2)Rh(L)_2]$ ($L_2 = (CO)_2$, COD, or TFB), only one isomer (**D**) was observed for $L_2 = (CO)_2$, whereas two isomers (**D** and **E**) were seen for L_2 = COD or TFB.[9] The size of the ancillary ligand on Rh had a clear influence on the stability of the two isomers and, for the smallest ligand, CO, the preference was clearly for isomer **D**, which allowed for a closer approach of the anionic Pt center to the cationic Rh center. Since the cationic $[Pd(C_6F_5)(4,4'\text{-}Me_2\text{-}bipy)]^+$ fragment is not expected to be bulkier than the anionic $[(C_6F_5)_3Pt]^-$ fragment (rather, it is probably smaller, taking into account the restrictions to rotation of the pentafluorophenyl rings already studied in ref 9), it seems that the attractive anion−cation forces in $[(C_6F_5)_3Pt(\mu\text{-}PPhPy_2)Rh(L)_2]$ and the repulsive cation−cation forces in $[Pd(C_6F_5)(4,4'\text{-}Me_2\text{-}bipy)(\mu\text{-}PPy_3)Rh(diolefin)](BF_4)_2$ may have some influence in the exclusive preference for conformation **E** found for the latter.

In the ^{19}F NMR spectra the complexes with $PPhPy_2$ as bridging ligand (**4** and **5**) show three 2:2:1 signals corresponding to a spin system A_2M_2XZ (where Z is the ^{31}P nucleus), showing that in solution the coordination plane of the palladium moiety is also a symmetry plane of the whole dication. The symmetry observed on the C_6F_5 group confirms that the structure of the cation in solution is that of an **E** conformer, since the same ^{19}F spectral pattern was found before in the **E** conformers of the zwitterionic complexes $[(C_6F_5)_3Pt(\mu\text{-}PPhPy_2)Rh(L)_2]$ ($L_2 = (CO)_2$, COD, or TFB), whereas all the ^{19}F nuclei of each C_6F_5 were non-equivalent in conformers **D**.[9] Moreover, four of the five ^1H nuclei of the phenyl ring are equivalent by pairs in complexes **4** and **5**, and only three cross-peaks are obtained in the $^1H-^{13}C$ HMQC experiment on the aromatic region. The ^1H olefin signals appear broadened in the spectrum of **4** at 25 °C in deuterated acetone due to the apparent rotation of the cyclooctadiene. This process is very often observed in diolefin rhodium(I) complexes, and it has been attributed to solvent coordination followed by Berry pseudorotation in the pentacoordinated intermediate but also to the dissociation of one ligand followed by a rearrangement in the tricoordinated intermediate.[12−14] In the complex with TFB as diolefin and BF_4^- as counteranion (**5a**) this exchange is faster and only one ^1H olefin signal is observed at 25 °C. Also in the ^{19}F NMR spectrum, the ^{19}F nuclei of TFB appear equivalent by pairs at room temperature. Although the tetrafluoroborate dicationic complexes are insoluble in most organic solvents, after exchanging the anion by BAF (BAF = tetrakis[3,5-bis(trifluoromethyl)phenyl]borate), the ^1H NMR in CD_2Cl_2 of complex **5b** could be registered, showing two olefinic signals for the TFB ligand, meaning that the olefin rotation in this solvent is slow. The rotation rate was measured by spin saturation transfer at 0 °C affording $k_{rot} = 1.8\ s^{-1}$ in pure CD_2Cl_2, and $k_{rot} = 3.9\ s^{-1}$ in a 9:1 mixture of CD_2Cl_2/acetone-d_6. Further increase in the ratio of acetone in the solvent mixture makes the exchange rate too fast to be

Table 3. Spectroscopic Data

compound	(isomer, %)	δ^{31}P (ppm)	δ ^{13}C[a] (ppm)	δ ^{13}C[b] (ppm)	δ ^{1}H[c] (ppm)	IR[d] (cm^{-1})
[Pd(C_6F_5)(4,4′-Me_2-bipy)(μ-PPhPy$_2$)Rh(COD)](BF_4)$_2$ (**4**)						1622
	(**E**, 100%)	49.61	156.5	90.5	9.92	1586
				85.7		1564
						1559(sh)
[Pd(C_6F_5)(4,4′-Me_2-bipy)(μ-PPhPy$_2$)Rh(TFB)](BF_4)$_2$	(**E**, 100%)	47.68	154.4[f]	64.6	9.73	1618
(**5a** or **5b**)				65.5[f]		1587
[Pd(C_6F_5)(4,4′-Me_2-bipy)(μ-PPy$_3$) Rh(COD)](BF_4)$_2$ (**6**)	(**E**, 100%)		156.6	92.2	9.93	1622
		47.92	156.1	84.9	9.78	1588
			152.2	89.8	8.11	1572
				87.3		
[(C_6F_5)(4,4′-Me_2-bipy)Pd(μ-PPy$_3$) Rh(TFB)](BF_4)$_2$	(**E**, 100%)		154.4[f]	65.8	9.70	1622
(**7a** or **7b**)		46.70	152.1[f]	67.0[f]	7.92	1590
						1574
						1564
[(C_6F_5)Au(μ-PPhPy$_2$)Rh(COD)](BF_4) (**10**)	(**D**, 100%)	34.66	154.2	92.4	7.33	1587
				87.8		
[(C_6F_5)Au(μ-PPhPy$_2$)Rh(TFB)](BF_4) (**11**)	(**D**, 100%)	35.81	155.3	69.9	7.65	1588
				66.0		
[(C_6F_5)Au(μ-PPy$_3$)Rh(COD)](BF_4) (**12**)	(**D**, 100%)	29.94	154.6	92.6	7.24	1589
			153.0	87.8	8.90	1575
[(C_6F_5)Au(μ-PPy$_3$)Rh(TFB)](BF_4) (**13**)	(**D**, 27%)	31.91	—[e]	—[e]	7.64	1583
					8.97	
	(**F**, 73%)	45.70	156.6	47.6	8.97	

[a] Chemical shift of the C6 from the 2-pyridyl group in PPhPy$_2$ ligand. [b] Chemical shift of olefinic carbons. [c] Chemical shift of the H3 from the 2-pyridyl group in PPh$_n$Py$_{3-n}$ ligand. [d] Nujol mull. [e] No data available due to low solubility. [f] In CD_2Cl_2 after exchanging the anion by BAF (that is, for **5b** or **7b**).

measured by this technique since extensive saturation transfer occurs during the selective excitation pulse. Line shape analysis in pure acetone as solvent afforded $k_{rot} = 55\ s^{-1}$ for **5b**, and $k_{rot} = 200\ s^{-1}$ for **5a**.[15] The observed dependence of the rotation rate with the solvent supports a major contribution of an associative mechanism involving coordination of acetone to give a pentacoordinated rhodium intermediate in which a isomerization process (such as Berry pseudorotation or turnstile) occurs. The small but non-negligible rotation rate value obtained in pure CD_2Cl_2 for **5b** suggests that, since BAF has a very low coordinating ability, a non-associative mechanism is simultaneously operating, possibly through the dissociation of a coordinated olefin. The contribution of traces of water or Cl^- to an associative mechanism in dichloromethane cannot be excluded, since these impurities are not easily removed. The effect of the counteranion is extremely difficult to foresee, since in dichloromethane the ions are expected to form ion pairs and the counteranion effect depends largely on the relative position of the anion and the cation.[16,17]

In complexes with PPy_3 as bridging ligand (**6** and **7**), the palladium coordination plane of Pd is not a symmetry plane due to the noncoordinated pyridyl group (Scheme 3, left). In the ^{1}H NMR spectra of [Pd(C_6F_5)(4,4′Me_2-bipy)(μ-PPy$_3$)-Rh(COD)](BF_4)$_2$ (**6**), at room temperature separate signals are obtained for the coordinated and noncoordinated P−Py groups, showing that the possible coordinated/noncoordinated Py exchange is a very slow process. At the same temperature, the cyclooctadiene signals coalesce due to olefin rotation. Finally, in the ^{19}F NMR spectrum at room temperature, the F_{ortho} atoms (F atoms ortho to the Pd−C bond) of the C_6F_5 group give two broad signals due to the slowness of Py rotation about the P−Py bond, which are well resolved in the spectrum at −10 °C. The slowness of P−P*y* rotation and Py exchange in **6** are in sharp contrast with the ease observed for the same processes in the same conformer **E** of [Pt(C_6F_5)$_3$-(μ-PPy$_3$)Rh(COD)],[9] which needs to be cooled below 203 K to stop the substitution and concurrent P−Py rotation. This difference can be understood considering the steric hindrance to coordination of the third P−Py group in complex **6**. This hindrance arises from the restriction to rotation of the pentafluorophenyl, imposed by the bipy ligand on Pd, which in turn is locked in the slot between the two coordinated P−Py groups (Scheme 3; this hindrance is very obvious for the analogous complex **4** in the space-filling representation in Figure 1, right). In the analogous complex [Pt(C_6F_5)$_3$(μ-PPy$_3$)Rh(COD)], the Pt(C_6F_5)$_3$ frame rotates freely about the P−Pt bond, and this make possible the P−Py rotation and its coordination to rhodium.

Scheme 3. Lowering of Symmetry by the Noncoordinated Py in Complex **6** (Left) and Hindrance to Coordination of the Third Py Group (Right)

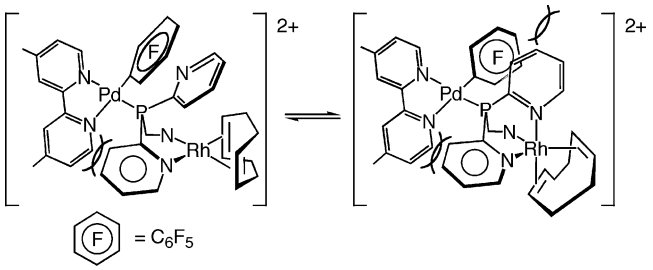

Complex [Pd(C_6F_5)(4,4′-Me_2-bipy)(μ-PPy$_3$)Rh(TFB)](BF_4)$_2$ (**7**) behaves similarly, but some processes are faster than for **6**. At 25 °C, there is no observable exchange between coordinated and noncoordinated P−Py groups, which give separate signals in the ^{1}H NMR spectrum. The rotation of the noncoordinated pyridyl about the P−Py bond is notice-

(16) Loupy, A.; Tchoubar, B. *Salt Effects in Organic and Organometallic Chemistry*; VCH: New York, 1995.
(17) Aullón, G.; Esquius, G.; Lledós, A.; Maseras, F.; Pons, J.; Ros, J. *Organometallics* **2004**, *23*, 5530−5539.

ably faster than for **6**, making equivalent the two coordinated P−Py groups at room temperature. In fact, this process has very low activation energy, and in order to slow the rotation and achieve the non-equivalence of the signals of the coordinated pyridyl groups, it is necessary to cool the sample to 186 K. Rotation of the diolefin is also observed, making equivalent the upper and lower halves of the TFB and is also faster than in complex **6**. This rotation, combined with the pyridine rotation, renders equivalent the four olefinic protons at room temperature. In the ^{1}H NMR at 187 K, the TFB protons give separate signals, and at higher temperatures, the signals coalesce, first due to the pyridine rotation (leading to left−right equivalence of the olefinic protons) and then due to the TFB rotation in the rhodium complex (leading to up−down equivalence of the nuclei on olefinic and on bridging carbons). The same two processes are observed more easily in the ^{19}F NMR spectra due to the larger chemical shift separations of the non-equivalent nuclei under slow exchange conditions. Above 223 K, the rotation of the noncoordinated Py renders equivalent the two F_{ortho} atoms of the C_6F_5 attached to palladium, while the pair of fluorine atoms of the TFB ligand coordinated to rhodium remain non-equivalent. The exchange rates have been measured by line shape analysis at 232.2 K.[15] At this temperature, the P−Py rotation rate is $k = 2.4 \times 10^3$ s^{-1} ($\Delta G^{\ddagger}_{232} = 41.3$ kJ mol^{-1}), and the TFB rotation rate is $k =$ 135 s^{-1} ($\Delta G^{\ddagger}_{232} = 46.8$ kJ mol^{-1}). The change of the anion BF_4^- for BAF yields a complex of the same cation but soluble in CD_2Cl_2. Their NMR spectra show that the cation $[Pd(C_6F_5)(4,4'\text{-}Me_2\text{-bipy})(\mu\text{-}PPy_3)Rh(TFB)]^+$ has very similar Py rotation rates in CD_2Cl_2 and in acetone-d_6: Also, the olefin rotation rate is very similar in the two solvents. In other words, contrary to the behavior observed for **5**, the dynamic processes are little influenced by the solvent or the anion. Then, this difference should be related to the existence of the third Py group. The olefin rotation can be satisfactorily explained assuming the coordination of the third Py group to give a pentacoordinate intermediate on which this rotation occurs. It is interesting to note that one might expect that this mechanism should produce also the equivalence of the three Py groups, as observed in closely related systems.[18] However, this is a special case where both the rotation of the third Py group around the Py−P bond and the rotation of the Pd coordination plane around the Pd−P bond are severely hindred by clash of the third Py group with the C_6F_5 group and the coordinated 4,4′-Me_2-bipy group with the two coordinated Py groups flanking it, respectively (see Scheme 3 and Figure 1, right)). For this reason, the third Py group never exchanges with the other two in the time scale of our experiments. This hindrance to rotation is comparable to that found for triptycene rotors, which have usually a very high activation energy, about 100 kJ mol^{-1}.[19]

The difference between complexes with TFB and COD toward the olefin rotation has also been observed in complexes $[Pt(C_6F_5)_3(\mu\text{-}PPy_3)Rh(diolefin)]$.[9]

Monocationic Complexes with the Fragment [Au-(C_6F_5)], 10−13. Complexes $[(C_6F_5)Au(\mu\text{-}PPhPy_2)Rh(diolefin)](BF_4)$ **10** (diolefin = COD), **11** (diolefin = TFB), and

Chart 2

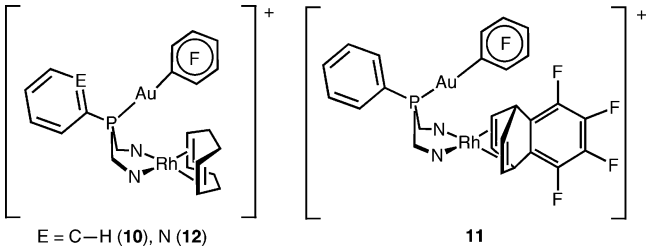

Scheme 4. Equilibrium between Isomers **D** and **F** of Complex **13**

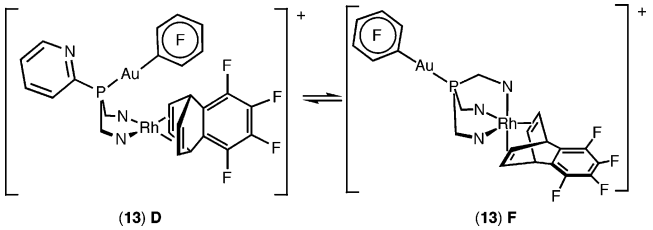

$[(C_6F_5)Au(\mu\text{-}PPy_3)Rh(COD)](BF_4)$ (**12**) show only conformation **D** (Chart 2).

In **10** and **11**, the phenyl group undergoes some restriction to rotation due to interactions with the two coordinated pyridyl groups, giving rise to broadening of the phenyl signals in their ^{1}H NMR spectra in $CDCl_3$ below 260 K due to the restricted rotation about the P−C bond. However, the phenyl signals were not resolved in the low-temperature limit for this solvent.

Complexes **10**−**12** do not undergo rotation of the diolefin coordinated to rhodium in $CDCl_3$, but in acetone-d_6, the rotation equilibrates the up and down halves of the diolefins at room temperature.

Complex **12** does not show exchange between the coordinated and noncoordinated pyridines in their spectra at 298 K. This is to be expected, as the substitution pathway requires change from **D** to **E** conformation and this, as observed in complex **13** (see below) and also in $[(C_6F_5)_3Pt(\mu\text{-}PPy_3)Rh(diolefin)]$, has high activation energy.[9]

The only compound in which two isomers are present in solution is $[(C_6F_5)Au(\mu\text{-}PPy_3)Rh(TFB)](BF_4)$ (**13**). The equilibrium is slow in $CDCl_3$ at 293 K and the ^{31}P, ^{19}F, and ^{1}H NMR spectra show signals from two isomers in a ratio **D**/**F** = 1:2.7 (Scheme 4). It is known for Tp′Rh−olefin complexes that κ^3-Tp′ compounds display the olefinic carbon signal at higher field than their κ^2-Tp′ analogues.[11b,20] A similar effect is found here, and the olefinic carbon signals of the major isomer of **13** (**F**) are shielded almost 20 ppm relative to the same signals of the square planar analogue with $PPhPy_2$, **11** (Table 3). The carbon signals from the minor isomer were too weak to be detected.

In the ^{1}H NMR spectra in acetone-d_6, the olefinic signals of **13** are in coalescence. While the major isomer (**F**) gives

(18) Fast interconversion is observed, for example, in complexes **7** and **8** in ref 9 (please note a mistake in the discussion on Py exchange in that paper, where complex **7E** is labeled as **6E**).

(19) (a) Kelly, T. R.; Tellitu, I.; Pérez Sestelo, J. *Angew. Chem., Int. Ed. Engl.* **1997**, *36*, 1866−1867. (b) Davis, A. P. *Angew. Chem., Int. Ed.* **1998**, *37*, 909−910. (c) Kelly, T. R.; Silva, R. A.; De Silva, H.; Jasmin, S.; Zhao, Y. *J. Am. Chem. Soc.* **2000**, *122*, 6935−6949.

(20) Del Ministro, E.; Renn, O.; Rüegger, H.; Venanzi, L. M.; Burckhardt, U.; Gramlich, V. *Inorg. Chim. Acta* **1995**, *240*, 631.

just one olefinic and one alkyl signal in all the temperature range, the minor one (**D**) shows two olefinic and two alkyl proton signals at 243 K. In the aromatic zone, the signals of the three pyridyl groups of isomer **F** are equivalent, while for the minor **D** isomer, the coordinated and noncoordinated pyridines give different signals. We have found that the chemical shift of the H3 proton of the coordinated pyridines is very sensitive to the conformation of the chelate ring, appearing in the range $\delta = 6.7-7.7$ ppm for **D** complexes, and $\delta > 9.5$ ppm for **E** complexes. The lower chemical shift for complexes **D** is probably due to the contribution of the diamagnetic effect of the noncoordinated aryl group located between the two H3 protons. The effect is quite general and has been also observed in complexes $[(C_6F_5)_3Pt(\mu\text{-}PPh_n\text{-}Py_{3-n})RhL_2]$.[9] For the minor isomer of complex **13**, the H3 protons of the coordinated pyridines appear at 7.6 ppm (Table 3), supporting a **D** structure. The EXSY (exchange spectroscopy) spectrum registered at 243 K with a mixing time of 0.4 s shows no cross-peaks due to pyridine substitution in **D** or exchange between isomers **D** and **F**; there are only cross-peaks correlating the olefinic signals of the **D** isomer due to olefin rotation. However, the same experiment at 273 K with mixing time of 0.6 s (the same T_1 measured by spin recovery) gave cross-peaks correlating signals of both isomers: the pyridyl groups of **F** exchange with both pyridyls of **D** (coordinated and noncoordinated). Considering the limited precision of this experiment, only the order of magnitude of the rate constant can be estimated, which is $1/T_1 \approx 1-10$ at this temperature.[21]

Conclusions

When there is no charge interaction, as in the (neutral gold)−rhodium bimetallic complexes, the preferred conformation directs the bulkiest P substituent toward the N-coordinated metal (rhodium), in a behavior comparable to that observed before for κ^2-Tp′ ligands.[8] An additional stabilization energy to give another conformation comes from the chelation of the third pyridine ring in complexes with PPy_3, as found in **13**, but this seems to depend largely on the electronic requirements of the rhodium center, since the pentacoordinate geometry is not found in complex **12**.

For complexes where the two metal centers are cationic, the electrical repulsion between them forces the metals to be as separate as possible. This has consequences on the conformation preferred (type **E**). The fact that there are no type **F** dicationic complexes seems to be the result of the particular geometry of the palladium frame chosen, which hinders the coordination of the third pyridine to the rhodium.

Experimental Section

General Methods. All reactions were carried out under N_2. Solvents were distilled using standard methods. The compounds $[Rh_2(\mu\text{-}Cl)_2(1,5\text{-}COD)_2]$,[22] $[Rh_2(\mu\text{-}Cl)_2(TFB)_2]$,[23] $PPhPy_2$,[24] PPy_3,[25] [AuCl(tht)],[26] $[Au(C_6F_5)(tht)]$,[26] $(NBu_4)_2[Pd_2(\mu\text{-}Br)_2(C_6F_5)_4]$,[27] $(NBu_4)_2[Pd_2(\mu\text{-}Br)_2Br_2(C_6F_5)_2]$,[28] $[Au(C_6F_5)(PPhPy_2)]$, and $[Au(C_6F_5)(PPy_3)]$[6b] were prepared by published methods. Combustion CHN analyses were made on a Perkin-Elmer 2400 CHN microanalyzer. IR spectra were recorded on a Perkin-Elmer FT 1720 X spectrophotometer.

NMR Spectra. ^1H NMR (300.16 MHz), ^{19}F NMR (282.4 MHz), ^{31}P NMR (121.4 MHz), and $^{13}C\{^1H\}$ (75.47 MHz) spectra were recorded on Bruker ARX 300 and AC 300 instruments equipped with a VT-100 variable-temperature probe. Chemical shifts are reported in ppm from $SiMe_4$ (^1H), CCl_3F (^{19}F), H_3PO_4 (85%) (^{31}P), or $K_2[PtCl_4]$ (1 M, D_2O) (^{195}Pt), with positive shifts downfield, at ambient probe temperature unless otherwise stated. *J* values are given in Hz. ^{13}C NMR were registered as $^1H-^{13}C$ correlation experiments, which were made with a HMQC sequence with BIRD selection and GARP decoupling during acquisition. Chemical shifts of quaternary carbons are not listed in the experimental data. The EXSY experiments were carried out with a standard NOESY program operating in phase sensitive mode, with a 5% random variation of the evolution time to avoid COSY cross-peaks. The saturation transfer experiments were carried out by using a 180° Gaussian-shaped soft pulse for the selective excitation of the desired signal, followed by a variable delay (10 values were used between 10^{-5} and 8 s) and a 90° nonselective pulse. The data analysis was carried out as described in the literature.[29]

Synthesis of the Complexes. $[Pd(C_6F_5)(Br)(4,4'\text{-}Me_2\text{-}bipy)]$ (1). To a stirred solution of $[Pd(\mu\text{-}Br)(Br)(C_6F_5)]_2(NBu_4)_2$ (2.0 g, 1.48 mmol) in CH_2Cl_2 (15 mL) was added solid 4,4′-dimethyl-2,2′-bipyridine (546 mg, 2.96 mmol). After 30 min, the product was precipitated by the addition of ethanol (80 mL) to give a yellow solid that was filtered, washed with ethanol and diethyl ether, and vacuum-dried. After being isolated, the product is almost insoluble in common solvents, precluding its characterization by NMR spectroscopy. Yield 1.56 g (98%). Anal. Calcd for $C_{18}H_{12}BrF_5N_2Pd$: C, 40.21; H, 2.25; N, 5.21. Found: C, 39.96; H, 2.32; N, 5.08. IR (Nujol mull, cm^{-1}): 1618 m, ν(CN).

$[Pd(C_6F_5)(4,4'\text{-}Me_2\text{-}bipy)(PPhPy_2)]BF_4$ (2). To a suspension of $[Pd(C_6F_5)(Br)(4,4'\text{-}Me\text{-}bipy)]$ (250.0 mg, 0.465 mmol) in acetone (80 mL) was added $AgBF_4$ (90.5 mg, 0.465 mmol) and $PPhPy_2$ (135.2 mg, 0.512 mmol). The solution was stirred for 24 h, protected from the light, and filtered through Celite. The solvent was evaporated and the residue was washed with 2-propanol, giving a white solid that was filtered and vacuum-dried. Yield 206.9 mg (55%). Anal. Calcd for $C_{34}H_{25}N_4BF_9PPd$: C, 50.49; H, 3.12; N, 6.93. Found: C, 50.45, H, 3.12 N, 6.50.^{31}P NMR (293 K, $CDCl_3$): δ 31.69. ^1H NMR (293 K, $CDCl_3$): δ 8.61 (m, 4H); 8.33 (m, 2H); 7.98 (m, 2H); 7.88 (m, 3H); 7.71 (m, 2H); 7.61 (m, 1H); 7.59 (m, 2H); 7.52 (d, 2H); 7.20 (d, 1H); 2.60 (s, 3H); 2.50 (s, 3H). ^{19}F NMR (293 K, $CDCl_3$): δ −161.83 (m, 2F); −159.40 (t, 1F); −150.44 (s, 4F, BF_4); −116.47 (m, 2F). IR (Nujol mull, cm^{-1}): 1619 (1627 shoulder) m, ν(CN); 1576 m, ν(CN).

$[Pd(C_6F_5)(4,4'\text{-}Me_2\text{-}bipy)(PPy_3)](BF_4)$ (3). Prepared as described for **2** but using PPy_3 (135.6 mg, 0.511 mmol) instead of $PPhPy_2$. Yield 450.1 mg (60%). Anal. Calcd for $C_{33}H_{24}N_5BF_9PPd$: C, 48.95; H, 2.99; N, 8.65. Found: C, 48.87; H, 3.04; N; 8.38. ^{31}P NMR (293 K, $CDCl_3$): δ 30.10. ^1H NMR (293 K, $CDCl_3$): 8.64 (m,

(21) Perrin, C.; Dwyer, T. J. *Chem. Rev.* **1990**, *90*, 935−937.
(22) Giordano, G.; Crabtree, R. H. *Inorg. Synth.* **1990**, *28*, 88.
(23) Roe, D. M.; Massey, A. G. *J. Organomet. Chem.* **1971**, *28*, 273.
(24) Newcome, G.; Hagen, D. C. *J. Org. Chem.* **1978**, *43*, 947−949. Xie, Y.; Lee, C.; Yang, Y.; Rettig, S. J.; James, B. R. *Can. J. Chem.* **1992**, *70*, 751.
(25) Kurtev, K.; Ribola, D.; Jones, R. A.; Cole-Hamilton, D. J.; Wilkinson, G. *J. C. S. Dalton.* **1980**, 55−58.
(26) Usón, R.; Laguna, A.; Laguna, M. *Inorg. Synth.* **1988**, *26*, 85.
(27) Usón, R.; Forniés, J.; Martínez, F.; Tomás, M. *J. Chem. Soc., Dalton Trans.* **1980**, 888.
(28) Usón, R.; Forniés, J.; Nalda, J. A.; Lozano, M. J.; Espinet, P.; Albéniz, A. C. *Inorg. Chim. Acta* **1989**, *156*, 251.
(29) Green, M. L. H.; Sella, A.; Wong, L.-L. *Organometallics* **1992**, *11*, 2650.

3H); 8.60 (s, 1H); 8.55 (s, 1H); 7.97 (m, 3H); 7.78 (m, 3H); 7.52 (m, 1H); 7.45 (m, 1H); 7.42 (m, 3H); 7.21 (d, 1H); 6.90 (d, 1H); 2.61 (s, 3H); 2.52 (s, 3H). ^{19}F NMR (293 K, $CDCl_3$): δ −162.02 (m, 2F); −159.40 (t, 1F-); −150.37 (s, 4F−BF_4); −116.43 (m, 2F). IR (Nujol mull, cm^{-1}): 1618 (1642sh) m, ν(CN); 1569 m, ν(CN).

[(4,4′-Me$_2$-bipy)(C$_6$F$_5$)Pd(μ-PPhPy$_2$)Rh(COD)](BF$_4$)$_2$ (4). To a stirred solution of [Rh$_2$(μ-Cl)$_2$(COD)$_2$] (45.9 mg, 0.093 mmol) in acetone (20 mL) was added $AgBF_4$ (36.2 mg, 0.186 mmol). After 30 min, the AgCl formed was filtered through Celite, and solid [Pd(C_6F_5)(4,4′-Me-bipy)(PPhPy$_2$)](BF$_4$) (150.0 mg, 0.186 mmol) was added to the yellow solution. The mixture was stirred for 20 min more, the solvent evaporated to dryness, and the residue stirred with 5 mL of thf (thf = tetrahydrofuran) affording a yellow solid that was filtered and vacuum-dried. The solid was recrystallized from CH_2Cl_2/ethanol. Yield 164.9 mg (80%). Anal. Calcd for $C_{42}H_{37}N_4B_2F_{13}PPdRh$: C, 45.58; H, 3.37; N, 5.06. Found: C, 45.79; H, 3.24; N, 4.94. ^{31}P NMR (293 K, $(CD_3)_2CO$): δ 49.61. ^{1}H NMR (293 K, $(CD_3)_2CO$): δ 9.84 (m, 2H); 9.40 (d, 2H); 8.67 (s, 1H); 8.58 (s, 1H); 8.29 (m, 2H); 7.96 (m, 2H); 7.88 (m, 1H); 7.75 (m, 1H); 7.62 (m, 4H); 7.53 (d, 1H); 6.93 (d, 1H); 6.72 (d, 1H); 2.61 (s, 3H); 2.43 (s, 3H). ^{19}F NMR (293 K, $(CD_3)_2CO$): δ −117.38 (m, 2F); −150.33 (s, 4F−BF_4); −158.45 (t, 1F); −160.10 (m, 2F). IR (Nujol mull, cm^{-1}): 1622 m, ν(CN); 1586 m, ν(CN); 1564 m, ν(CN); 1559, ν(CN).

[(4,4′-Me$_2$-bipy)(C$_6$F$_5$)Pd(μ-PPhPy$_2$)Rh(TFB)](BF$_4$)$_2$ (5a). Prepared as described for **4** but using [Rh$_2$(μ-Cl)$_2$(TFB)$_2$] (67.8 mg, 0.093 mmol) instead of [Rh$_2$(μ-Cl)$_2$(COD)$_2$]. Yield 166.5 mg (73%). Anal. Calcd for $C_{46}H_{31}N_4B_2F_{17}PPdRh$: C, 45.12; H, 2.55; N, 4.57. Found: C, 45.20; H, 2.80; N, 4.39. ^{31}P NMR (293 K, $(CD_3)_2CO$): δ 47.68. ^{1}H NMR (293 K, $(CD_3)_2CO$): δ 9.73 (t, 2H, H-3-Py$_{coord}$); 9.12 (d, 2H, H-6-Py$_{coord}$); 8.70 (s, 1H, 4,4′-Me$_2$-bipy); 8.63 (s, 1H, 4,4′-Me$_2$-bipy); 8.29 (m, 2H, H-4-Py$_{coord}$); 7.99 (m, 1H, Ph); 7.91 (m, 3H, H-5-Py$_{coord}$); 7.91 (m, 1H, 4,4′-Me$_2$-bipy); 7.76 (m, 2H, Ph); 7.48 (m, 4H, Ph); 7.48 (m, 4H, 4,4′-Me$_2$-bipy); 7.03 (d, 1H, 4,4′-Me$_2$-bipy); 5.13 (m, broad, 2H-TFB); 4.00 (s, broad, 4H-TFB); 2.61 (s, 3H, 4,4′-Me$_2$-bipy); 2.47 (s, 3H, 4,4′-Me$_2$-bipy). ^{19}F NMR (293 K, $(CD_3)_2CO$): δ −160.11 (m, 2F); −160.11 (m, 2F); −117.53 (d, 2F); −158.12 (m, 1F); −150.46 (s, 4F−BF_4); −147.11 (d, 2F). IR (Nujol mull, cm^{-1}): 1618 ν(CN); 1587 ν(CN).

Preparation of a Solution of [(4,4′-Me$_2$-bipy)(C$_6$F$_5$)Pd(μ-PPhPy$_2$)Rh(TFB)] [B(3,5-C$_6$H$_3$(CF$_3$)$_2$)$_4$]$_2$ (5b). To a solution of **5** (15 mg, 0.012 mmol) in acetone was added NaBAF (24 mg, 0.027 mmol); the resulting solution was filtered to remove $NaBF_4$, and the solvent was evaporated. The residue was dissolved in ether, filtered again, and evaporated to dryness, giving a residue that was insoluble in $CDCl_3$ but quite soluble in CD_2Cl_2.

[(4,4′-Me$_2$-bipy)(C$_6$F$_5$)Pd(μ-PPy$_3$)Rh(COD)](BF$_4$)$_2$ (6). Prepared as described for **4** but using [Pd(C_6F_5)(4,4′-Me$_2$-bipy)(PPy$_3$)](BF$_4$) (150.0 mg, 0.185 mmol) instead of [Pd(C_6F_5)(4,4′-Me-bipy)(PPhPy$_2$)](BF$_4$). Yield 147.1 mg (72%). Anal. Calcd for $C_{41}H_{36}N_5B_2F_{13}PPdRh$: C, 44.46; H, 3.28; N, 6.32. Found: C, 44.12; H, 3.17; N, 6.10. ^{31}P NMR (293 K, $(CD_3)_2CO$): δ 47.92. ^{1}H NMR (293 K, $(CD_3)_2CO$): δ 9.78 (broad, 2H); 9.34 (d, 2H); 8.74 (d, 1H); 8.66 (s, 4,4′-Me$_2$-bipy, 1H); 8.57 (s, 4,4′-Me$_2$-bipy, 2H); 8.26 (m, 2H); 8.07 (m, 2H); 7.95 (m, 2H); 7.82 (m, 4,4′-Me$_2$-bipy, 1H); 7.69 (m, 1H); 7.51 (d, 4,4′-Me$_2$-bipy, 1H); 6.92 (d, 4,4′-Me$_2$-bipy, 1H); 6.78 (m, 4,4′-Me$_2$-bipy, 1H); 2.59 (s, 4,4′-Me$_2$-bipy, 3H); 2.41 (s, 4,4′-Me$_2$-bipy, 3H). ^{19}F NMR (293 K, $(CD_3)_2CO$): δ −160.56 (m, 2F); −158.14 (m, 1F); −150.26(s, 4F-TFB); −117.42 (broad, 1F); −115.83 (broad, 1F). IR (Nujol mull, cm^{-1}): 1622 ν(CN); 1588 ν(CN); 1572 ν(CN).

[(4,4′-Me$_2$-bipy)(C$_6$F$_5$)Pd(μ-PPy$_3$)Rh(TFB)](BF$_4$)$_2$ (7). Prepared as **4** but using [Rh$_2$(μ-Cl)$_2$(TFB)$_2$] (67.1 mg, 0.092 mmol) instead of [Rh$_2$(μ-Cl)$_2$(COD)$_2$] and [Pd(C_6F_5)(4,4′-Me-bipy)(PPy$_3$)](BF$_4$) (150.0 mg, 0.185 mmol) instead of [Pd(C_6F_5)(4,4′-Me$_2$-bipy)(PPhPy$_2$)](BF$_4$). Yield: 125.4 mg (55%). Anal. Calcd for $C_{45}H_{30}N_5B_2F_{17}PPdRh$: C, 44.10; H, 2.47; N, 5.71. Found: C, 43.93; H, 2.64; N, 5.60. ^{31}P NMR (293 K, $(CD_3)_2CO$): δ 46.70. ^{1}H NMR (293 K, $(CD_3)_2CO$): δ 9.70 (t, 2H, H-3-Py$_{coord}$); 9.08 (d, 2H, H-6-Py$_{coord}$); 8.86 (d, 1H, H-6-Py$_{noncoord}$); 8.72 (s, 1H, 4,4′-Me$_2$-bipy); 8.63 (s, 1H, 4,4′-Me$_2$-bipy); 8.30 (t, 3H, H-4-Py$_{coord}$); 8.30 (t, 3H, H-3-Py$_{noncoord}$); 8.06 (m, 1H, H-4-Py$_{noncoord}$); 7.92 (m, 1H, 4,4′-Me$_2$-bipy); 7.92 (m, 3H, H-5-Py$_{coord}$); 7.83 (m, 1H, H-5-Py$_{noncoord}$); 7.56 (d, 2H, 4,4′-Me$_2$-bipy); 7.05 (d, 1H, 4,4′-Me$_2$-bipy); 5.22 (m, broad, TFB); 4.05 (m, broad, 4H-TFB); 2.60 (s, 3H, 4,4′-Me$_2$-bipy); 2.50 (s, 3H, 4,4′-Me$_2$-bipy); 1.30 (m, broad, 2H-TFB). ^{19}F NMR (293 K, $(CD_3)_2CO$): δ −160.48 (m, 2F); −160.03 (m, 2F-TFB); −157.83 (m, 1F); −150.43 (s, 4F−BF_4); −146.95 (d, 2F-TFB); −116.77 (d, 2F). ^{31}P NMR (310K, $(CD_3)_2CO$): δ 50.89. IR (Nujol mull, cm^{-1}): 1622 ν(CN); 1590 ν(CN); 1574 ν(CN); 1564 ν(CN). To register NMR spectra in CD_2Cl_2, the anion BF_4 was exchanged with BAF following the same procedure described above for **5**.

[(C$_6$F$_5$)Au(μ-PPhPy$_2$)Rh(COD)](BF$_4$) (10). To a stirred solution of [Rh$_2$(μ-Cl)$_2$(COD)$_2$] (115.0 mg, 0.233 mmol) in 15 mL of acetone was added solid $TlBF_4$ (135.9 mg, 0.466 mmol). After 30 min, [Au(C_6F_5)(PPhPy$_2$)] (293.0 mg, 0.466 mmol) was added to the solution. The mixture was stirred for 30 min more, the TlCl formed was filtered through Celite, and the solvent was evaporated to 5 mL. The addition of ethanol (20 mL) and further evaporation of the remaining acetone gave the product as a yellow crystalline solid that was filtered and vacuum-dried. Yield 334.0 mg (77%). Anal. Calcd for $C_{30}H_{25}N_2AuBF_9PRh$: C, 38.91; H, 2.72; N, 3.02. Found: C, 38.67; H, 2.75, N, 2.96. ^{31}P NMR (293 K $CDCl_3$) δ : 34.55. ^{1}H NMR (293 K $CDCl_3$): δ 4.50 (m, 2H-olefin); 4.27 (m, 2H-olefin); 2.98 (m, 2H); 2.51 (m, 2H); 2.18 (m, 2H); 1.90 (m, 2H). ^{19}F NMR (293 K $CDCl_3$): δ −164.5 (tdt, 2F); −160.42 (t, 1F); −156.92 (s, 4F); −119.52 (d, 2F). IR (Nujol mull, cm^{-1}): 1587 ν(CN).

[(C$_6$F$_5$)Au(μ-PPhPy$_2$)Rh(TFB)](BF$_4$) (11). Prepared as **10** but using [Rh$_2$(μ-Cl)$_2$(TFB)$_2$] (173.0 mg, 0.234 mmol) instead of [Rh$_2$(μ-Cl)$_2$(COD)$_2$]. Yield 370.0 mg (74%). Anal. Calcd for $C_{34}H_{19}N_2AuBF_{13}PRh$: C, 39.11; H, 1.82; N, 2.68. Found: C, 38.96; H, 1.88; N, 2.77. ^{31}P NMR (293 K $(CD_3)_2CO$): δ 36.39. ^{1}H NMR (293 K $(CD_3)_2CO$): δ 9.12 (d, 2H); 8.45 (m, 2H); 8.10 (m, 3H); 7.99 (m, 2H); 7.76 (m, 2H); 7.65 (m, 2H); 6.31 (broad, 1H); 5.63 (broad, 1H); 4.87 (broad, 2H); 4.57 (broad, 2H). IR (Nujol mull, cm^{-1}): 1588 ν(CN).

[(C$_6$F$_5$)Au(μ-PPy$_3$)Rh(COD)](BF$_4$) (12). Prepared as **10** but using [Rh$_2$(μ-Cl)$_2$(COD)$_2$] (117.6 mg, 0.238 mmol), $TlBF_4$ (139.0 mg, 0.477 mmol), and [Au(C_6F_5)(PPy$_3$)] (300.0 mg, 0.477 mmol) instead of [Au(C_6F_5)(PPhPy$_2$)]. Yield 295.0 mg (67%). Anal. Calcd for $C_{29}H_{24}N_3AuBF_9PRh$: C, 37.57; H, 2.60; N, 4.53. Found: C, 37.38; H, 2.83; N, 4.33. ^{31}P NMR (293 K $CDCl_3$): δ 29.94. ^{1}H NMR (293 K $CDCl_3$): δ 9.09 (d, 2H, H-6-Py$_{coord}$); 9.00 (d, 1H, H-6-Py$_{noncoord}$); 8.90 (t, 1H, H-3-Py$_{noncoord}$); 8.20 (m, 1H, H-4-Py$_{noncoord}$); 7.84 (m, 2H, H-4-Py$_{coord}$); 7.80 (m, 1H, H-5-Py$_{noncoord}$); 7.64 (t, 2H, H-5-Py$_{coord}$); 7.24 (m, 2H, H-3-Py$_{coord}$); 4.58 (m, 2H-olefin); 4.32 (m, 2H-olefin); 3.02 (m, 2H); 2.52 (m, 2H); 2.14 (m, 2H); 1.90 (m, 2H). ^{19}F NMR (293 K $CDCl_3$): δ −165.40 (t, 2F); −159.95 (t, 1F); −156.36 (s, 4F, BF_4); −119.48 ppm (d, 2F). ^{13}C NMR (293 K $CDCl_3$): δ 154.6 (C-6-Py$_{coord}$); 153.0 (C-6-Py$_{noncoord}$); 138.8 (C-4-Py$_{coord}$); 138.3 (C-4-Py$_{noncoord}$); 137.6 (C-3-Py$_{noncoord}$); 130.8 (C-3-Py$_{coord}$); 128.5 (C-5-Py$_{noncoord}$); 127.7 (C-5-Py$_{coord}$); 92.6 (C-olefin); 87.9 (C-olefin); 32.1 (COD); 29.8 (COD). IR (Nujol mull, cm^{-1}): 1589 ν(CN); 1575 ν(CN).

[(C$_6$F$_5$)Au(μ-PPy$_3$)Rh(TFB)](BF$_4$) (13). Prepared as **12** but using [Rh$_2$(μ-Cl)$_2$(TFB)$_2$] (174.0 mg, 0.240 mmol) instead of [Rh$_2$-

Table 4. Data of the X-ray Diffraction Studies

compound	**4**·Me_2CO	**11**
	Crystal Data	
empirical formula	$C_{45}H_{43}B_2F_{13}N_4OPPdRh$	$C_{34}H_{19}AuBF_{13}N_2PRh$
fw	1164.73	1044.17
cryst syst	monoclinic	triclinic
space group	$P2_1/c$	$P\bar{1}$
a (Å)	10.9644(14)	10.2401(11)
b (Å)	22.662(3)	10.2403(11)
c (Å)	19.628(3)	16.5327(18)
α (deg)	90	93.909(2)
β (deg)	103.981(3)	106.585(2)
γ (deg)	90	92.388(2)
V (Å^3)	3830.4(18)	1654.3(3)
Z	4	2
D_{calc} (g cm^{-3})	1.635	2.096
absorption coefficient (mm^{-1})	0.853	5.080
F(000)	2328	996
cryst size (mm^3)	0.25 × 0.08 × 0.08	0.24 × 0.06 × 0.06
	Data Collection	
temp (K)	298(2)	300(2)
θ range for data collection	1.40−23.27°	1.57−23.27°
wavelength (Å)	0.71073 (Mo K$_\alpha$)	0.71073 (Mo K$_\alpha$)
index ranges	$-12 \le h \le 11$	$-11 \le h \le 10$
	$0 \le k \le 25$	$-11 \le k \le 11$
	$0 \le l \le 21$	$0 \le l \le 18$
reflns collected	17 484	7737
independent reflns	6724 (R_{int} = 0.0506)	4742 (R_{int} = 0.0284)
completeness to θ	23.27° (98.8%)	23.28° (99.4%)
	Refinement	
absorption correction	SADABS	SADABS
max. and min. transmission	1.000000 and 0.777393	1.000000 and 0.582875
data/restraints/params	6724/0/682	4742/0/478
GOF on F^2	0.993	1.029
final R indices [$I > 2\sigma(I)$]	R1 = 0.0375, wR2 = 0.0552	R1 = 0.0374, wR2 = 0.0945
R indices (all data)	R1 = 0.0766, wR2 = 0.0613	R1 = 0.0471, wR2 = 0.1058
largest diff. peak and hole (e Å^{-3})	0.451 and −0.482	1.033 and −1.341

(μ-Cl)$_2$(COD)$_2$]. Yield 330.0 mg (66%). Anal. Calcd for $C_{33}H_{18}N_3AuBF_{13}PRh$: C, 37.91; H, 1.72; N, 4.02. Found: C, 37.53; H, 1.80; N, 3.90. ^{31}P NMR (293 K $(CD_3)_2CO$): δ 46.47 (major isomer, 73%); 32.03 (minor isomer 27%). ^{1}H NMR (293 K $(CD_3)_2CO$): δ 9.63 (d, 3H); 9.08 (d, 3H); 8.96 (m, 4H); 8.43 (m, 4H); 8.09 (broad, 3H); 7.94 (broad, 3H); 7.68 (d, 4H); 6.29 (s, broad, 1H); 5.96 (s, 2H); 5.60 (s, broad, 1H); 4.87 (s, broad, 2H); 4.58 (s, broad, 2H); 3.91 (s, 4H. ^{19}F NMR (293 K $(CD_3)_2CO$): δ −162.31 (2F-major); −161.75 (2F-minor); −160.46 (2F− major); −159.96 (2F− minor); −157.76 (1F− major and 1F− minor); −150.41 (4F− major and 4F− minor); −148.33 (1F− minor); −147.33 (2F− major); −147.00 (broad, 1F− minor); −115.27 (2F− major); −114.49 (2F− minor). IR (Nujol mull, cm^{-1}): 1583 m, ν(CN). IR (CH_2Cl_2 solution, cm^{-1}): 1587 and 1572, ν(CN).

Experimental Procedure for X-ray Crystallography. Suitable single crystals were mounted on glass fibers, and diffraction measurements were made using a Bruker SMART CCD area-detector diffractometer with Mo Kα radiation (λ = 0.71073 Å).[30] Intensities were integrated from several series of exposures, each exposure covering 0.3° in ω, the total data set being a hemisphere.[31] Absorption corrections were applied, based on multiple and symmetry-equivalent measurements.[32] The structure was solved by direct methods and refined by least squares on weighted F^2 values for all reflections (see Table 4).[33] All non-hydrogen atoms were assigned anisotropic displacement parameters and refined without positional constraints. Hydrogen atoms were taken into account at calculated positions, and their positional parameters were refined. Both BF_4 counteranions in compound **4**·Me_2CO were disordered. Refinement proceeded smoothly to give R1 = 0.0375 for **4**·Me_2CO and R1 = 0.0374 for **11** based on the reflections with $I > 2\sigma(I)$. Complex neutral-atom scattering factors were used.[34] Crystallographic data (excluding structure factors) for the structures **4**·Me_2CO and **11** reported in this paper have been deposited with the Cambridge Crystallographic Data Centre as Supplementary publication nos. CCDC-293670 and CCDC-293671. Copies of the data can be obtained free of charge on application to the CCDC, 12 Union Road, Cambridge CB2 1EZ, U.K. [Fax: (internat.) + 44−1223/336−033; Email: deposit@ccdc.cam.ac.uk].

Acknowledgment. Financial support by the Ministerio de Educación y Ciencia (Project No. CTQ2004-07667/BQU) and the Junta de Castilla y León (Project No. VA 060/04) is very gratefully acknowledged.

Supporting Information Available: Additional NMR data and selected NMR spectra. This material is available free of charge via the Internet at http://pubs.acs.org.

IC0600477

(30) *SMART*, v 5.051; Bruker Analytical X-ray Instruments, Inc.: Madison, WI, 1998.
(31) *SAINT*, v 6.02; Bruker Analytical X-ray Instruments, Inc.: Madison, WI, 1999.
(32) Sheldrick, G. M. *SADABS: A Program for Absorption Correction with the Siemens SMART System*; University of Göttingen: Göttingen, Germany, 1996.
(33) *SHELXTL program system version 5.1*; Bruker Analytical X-ray Instruments, Inc.: Madison, WI, 1998.
(34) *International Tables for Crystallography*; Kluwer: Dordrecht, 1992; Vol. C.